Photocatalytic water oxidation by persulphate with a Ca^{2+} ion-incorporated polymeric cobalt cyanide complex affording O_2 with 200% quantum efficiency

Yusuke Yamada, Kohei Oyama, Tomoyoshi Suenobu, Shunichi Fukuzumi

Citation	Chemical Communications. 53(24); 3418-3421.
Issue Date	2017-03-25
Type	Journal Article
Textversion	Author
Supplementary files	Supplementary information is available at https://doi.org/10.1039/C7CC00199A
Rights	The following article appeared in Chemical Communications, 2017, 53, 3418-3421 and may be found at https://doi.org/10.1039/C7CC00199A. This is the accepted manuscript version. Please cite only the published version. この論文は出版社版でありません。引用の際には出版社版をご確認ご利用ください。
DOI	10.1039/C7CC00199A

Yamada, Y., Oyama, K., Suenobu, T., & Fukuzumi, S. (2017). Photocatalytic water oxidation by persulphate with a Ca2+ ion-incorporated polymeric cobalt cyanide complex affording O2 with 200% quantum efficiency. Chemical Communications. 53, 3418–3421. https://doi.org/10.1039/c7cc00199a

Journal Name

COMMUNICATION

Photocatalytic water oxidation by persulphate with a Ca^{2+} ion-incorporated polymeric cobalt cyanide complex affording O_2 with 200% quantum efficiency

Received 00th January 20xx,
Accepted 00th January 20xx

DOI: 10.1039/x0xx00000x

www.rsc.org/

Yusuke Yamada,*[a] Kohei Oyama,[b] Tomoyoshi Suenobu[b] and Shunichi Fukuzumi*[cd]

Incorporation of a small amount of Ca^{2+} ion into a polymeric Co cyanide complex to form $Ca_x[Co^{II}(H_2O)_2]_{1.5-x}[Co^{III}(CN)_6]$ resulted in significant enhancement of activity for photocatalytic water oxidation in an aqueous solution (pH 7.0) using $[Ru(bpy)_3]^{2+}$ (bpy = 2,2'-bipyridine) as a photocatalyst and $Na_2S_2O_8$ as as an electron acceptor to achieve 200% quantum efficiency.

Development of highly active water oxidation catalysts has been strongly demanded, because a water oxidation catalyst is a crucial piece to construct an artificial photosynthetic system composed of light-harvesting and charge-separation units, and a proton or CO_2 reduction catalyst.[1-3] In natural systems, photocatalytic water oxidation is solely performed by the Ca^{2+} ion-incorporated Mn_4O_5 cluster, which acts as the oxygen evolving complex (OEC) in photosystem II.[4] Although the essential role of the Ca^{2+} ion is still disputed,[5-8] incorporation of Ca^{2+} ion to an artificial water-oxidation catalyst such as manganese oxides has been reported to result in improvement of the catalytic activity for water oxidation.[9-11] Not only Ca^{2+} ion but also other redox inactive metal ions have been reported to act as Lewis acids to enhance the catalytic redox activity.[12,13] Redox inactive metal ions can readily interact with oxo or peroxo species, regulating the water-oxidation activity.[14] However, the effects of Ca^{2+} ion and other metal ions interacting with water molecules, which coordinate to catalytically active metal ions for water oxidation, have yet to be clarified.

There have been extensive studies on the photocatalytic water oxidation by persulphate ($S_2O_8^{2-}$) with $[Ru(bpy)_3]^{2+}$ (bpy = 2,2'-bipyridine) as a photocatalyst using various homogeneous and heterogeneous water oxidation catalysts (WOCs) as shown in Scheme 1.[15] The O_2 yield based on two equivalents of persulphate (maximum 100%) is normally less than 50% because the ligand of $[Ru(bpy)_3]^{3+}$ produced during the photocatalytic water oxidation was oxidised under basic conditions in competition with the catalytic water oxidation.[15] The quantum efficiency in the case of photocatalytic water oxidation is defined as (number of holes / s)/(number of photons / s), because holes are produced instead of electrons. On the other hand, two equivalents of $[Ru(bpy)_3]^{3+}$ are produced by photoinduced electron transfer from the excited state of $[Ru(bpy)_3]^{2+}$ ($[Ru(bpy)_3]^{2+*}$: * denotes the excited state) to $S_2O_8^{2-}$, because the electron-transfer reduction of $S_2O_8^{2-}$ results in formation of SO_4^{2-} and $SO_4^{\bullet-}$, the latter of which can oxidise another $[Ru(bpy)_3]^{2+}$ to $[Ru(bpy)_3]^{3+}$.[15-17] In such a case the maximum quantum efficiency of $[Ru(bpy)_3]^{3+}$ formation is 200% as reported previously.[17] The maximum quantum efficiency of O_2 evolution in Scheme 1 should also be 200%, which has, however, never been achieved so far.

Recently, a polymeric Co cyanide complex, $[Co^{II}(H_2O)_2]_{1.5}[Co^{III}(CN)_6]$, has been reported to act as an efficient WOC.[18-20] In the complex, the one third of the crystallographically equivalent positions for the $[Co^{III}(CN)_6]^{3-}$ unit are vacant, because the number of Co^{II} ion is 1.5 times larger than that of Co^{III} ion due to charge compensation. The defect sites can form "water nests" suitable for incorporating Lewis acid metal ions with interaction through water molecules coordinating to Co^{II} ions (Fig. 1). Thus, the polymeric Co cyanide complexes are suitable scaffold to examine the

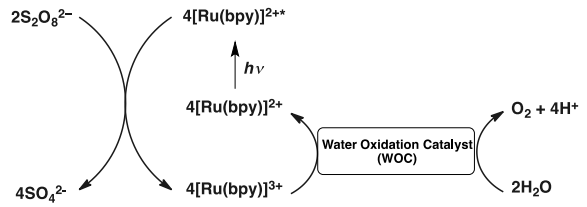

Scheme 1 Overall catalytic cycle of visible-light driven water oxidation

[a] Department of Applied Chemistry and Bioengineering, Graduate School of Engineering, Osaka City University, Osaka 558-8585, Japan. E-mail: ymd@a-chem.eng.osaka-cu.ac.jp
[b] Department of Material and Life Science, Graduate School of Engineering, Osaka University, SENTAN, Japan Science and Technology Agency (JST), Suita, Osaka 565-0871, Japan.
[c] Department of Chemistry and Nano Science, Ewha Womans University, Seoul 120-750, Korea. E-mail: fukuzumi@chem.eng.osaka-u.ac.jp
[d] Faculty of Science and Engineering, Meijo University, SENTAN, Japan Science and Technology Agency (JST), Nagoya, Aichi 468-8502, Japan.

† *Electronic Supplementary Information (ESI) available: Experimental details, TG/DTA (Fig. S1), XPS depth profiles (Fig. S2), DLS (Fig. S3), TEM (Figs. S4, S7), XRD (Figs. S5, S13), IR (Figs. S6, S14), Time courses of O_2 evolution (Figs. S8, S9, S11,12,15) and UV-vis absorption spectra (Fig. S10). See DOI: 10.1039/x0xx00000x*

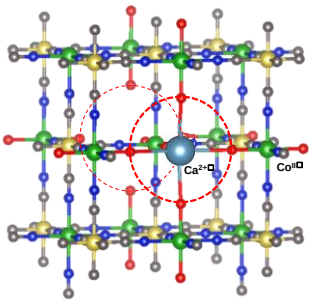

Fig. 1 A schematic drawing of $Ca_x[Co^{II}(H_2O)_2]_{1.5-x}[Co^{III}(CN)_6]$. Elements are colour-coded: Co^{III} (yellow), C (gray), N (blue), Co^{II} (green), O (red), Ca (cyan). H atoms of water molecules are omitted for clarity. Red broken circles indicate "water nests".

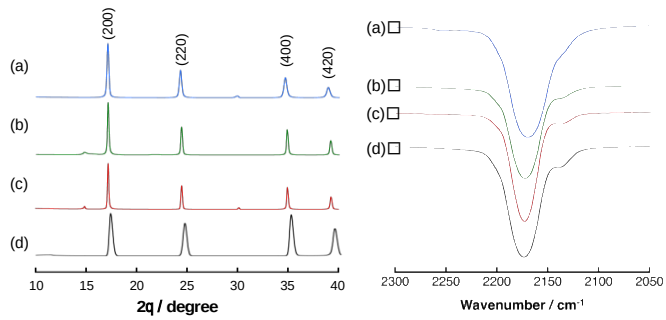

Fig. 2 Powder X-ray diffraction patterns (left) and IR spectra (right) of $Ca_x[Co^{II}(H_2O)_2]_{1.5-x}[Co^{III}(CN)_6]$, [x = (a) 0.37, (b) 0.14, (c) 0.06 and (d) 0].

incorporation effect of Ca^{2+} ion or other Lewis acids on the water oxidation catalysis of N-bound Co^{II} ions. The structural difference induced by incorporation of Ca^{2+} ion was examined by powder X–ray diffractions (XRD), spectroscopic methods including IR, and depth profile analysis by X-ray photoelectron spectroscopy (XPS). The catalytic activity of the Co cyanide complexes for visible-light driven water oxidation was investigated by the addition of other redox-inactive metal ions.

Polymeric Co cyanide complexes incorporating Ca^{2+} ion were obtained as precipitates by dropping an aqueous solution of $H_3[Co^{III}(CN)_6]$ to that of $Co(NO_3)_2$ and $Ca(NO_3)_2$ at room temperature. The compositions of the prepared complexes determined by X-ray fluorescence (XRF) measurements indicated that Ca^{2+} contents varied from x = 0.06 to 0.37 in the formula of $Ca_x[Co^{II}(H_2O)_2]_{1.5-x}[Co^{III}(CN)_6]$ depending on the concentrations of Ca^{2+} ion in solutions (Table S1†). Thermogravimetric analysis indicated that each complex contained 12-16 water molecules per the monomer unit irrespective of Ca^{2+} contents (Fig. S1†). In contrast, depth profile analyses of O1s peak areas by XPS indicate that the amounts of water molecules beneath the surfaces increased by incorporation of Ca^{2+} ion (Fig. S2†). Particles sizes were determined by dynamic light scattering (DLS) and TEM measurements (Figs. S3 and S4†), suggesting that incorporation of Ca^{2+} ion mainly effects on aggregability of the particles. Bimodal size distribution at DLS measurements was observed only for $[Co^{II}(H_2O)_2]_{1.5}[Co^{III}(CN)_6]$ although the sizes of primary nanoparticles are smaller than 100 nm as evidenced by TEM observations. The high aggregability results from charge-neutralized surfaces of the nanoparticles owing to the inertness of N-bound Co^{II} ion. In contrast, lower aggregability of nanoparticles of the complexes incorporating Ca^{2+} ion may result from negatively charged surfaces due to partial dissociation of labile Ca^{2+} ion. The XRD peaks of the complexes were indexed to the cubic structure, which is characteristic for Prussian blue analogues (Fig. 2).[21] There are two possibilities for the positions of Ca^{2+} ions in the crystals; one is the defect sites and the other is substitution of N-bound Co^{II} ion. The difference in lattice parameters determined by the (200) diffraction peaks of the complexes (10.21 and 10.35 Å for the complexes with x = 0 and 0.37, respectively) was within 1.5%, although Ca^{2+} ion (1.14 Å) is much larger than Co^{II} ion (0.79 Å).[22] The structures of the obtained Co complexes were also investigated by IR spectroscopy, because the wavenumbers of CN stretching bands, ν(CN), keenly reflect local coordination environments of the CN ligand.[23] The ν(CN) of $Ca_x[Co^{II}(H_2O)_2]_{1.5-x}[Co^{III}(CN)_6]$ with x = 0, 0.06 and 0.14 appeared at 2170 cm^{-1} and that of $Ca_{0.37}[Co^{II}(H_2O)_2]_{1.13}[Co^{III}(CN)_6]$ appeared at 2173 cm^{-1} (Fig. 2). The shift smaller than 3 cm^{-1} suggested that the interaction between a CN ligand and a Ca^{2+} ion is negligible. Thus, incorporated Ca^{2+} ions mainly occupy the defect sites interacting with water molecules, which coordinate to N-bound Co^{II} ions acting as active sites for water oxidation.

The other Co cyanide complexes incorporating redox-inactive metal ion were prepared by the same method used for $Ca_x[Co^{II}(H_2O)_2]_{1.5-x}[Co^{III}(CN)_6]$. The contents of Mg^{2+} and Sc^{3+} ions were determined by XRF (Tables S2 and S3†) and the cubic structures of Prussian blue analogues were confirmed by XRD (Fig. S5†). The complexes were further characterised by IR and TEM measurements (Figs. S6 and S7†). No significant shift in ν(CN) was observed by incorporation of Mg^{2+} and Sc^{3+} ions in IR spectra.

Photocatalytic O_2 evolution was conducted by visible-light irradiation (λ > 420 nm) of a phosphate buffer (2.0 mL, 50 mM, pH 7.0) containing Co cyanide complex incorporating a redox-inactive metal ion as a WOC (80 µg, $Ca_{0.06}[Co^{II}(H_2O)_2]_{1.44}[Co^{III}(CN)_6]$, $Sc_{0.08}[Co^{II}(H_2O)_2]_{1.38}[Co^{III}(CN)_6]$, $Mg_{0.05}[Co^{II}(H_2O)_2]_{1.45}[Co^{III}(CN)_6]$, or $[Co^{II}(H_2O)_2]_{1.50}[Co^{III}(CN)_6]$), $[Ru(bpy)_3]^{2+}$ (1.0 mM) as a photocatalyst, $Na_2S_2O_8$ (5.0 mM) as a sacrificial electron acceptor. The amount of Co leached from the complexes during the reaction was negligible as confirmed by atomic absorption spectroscopy. Time courses of O_2 evolution (Fig. 3) indicated that incorporation of redox-inactive metal ions enhanced the catalytic activity of$[Co^{II}(H_2O)_2]_{1.5}[Co^{III}(CN)_6]$ in terms of an O_2-evolution rate and an O_2 yield based on the stoichiometry of the water oxidation by $Na_2S_2O_8$ ($2Na_2S_2O_8 + 2H_2O \rightarrow 2Na_2SO_4 + 2H_2SO_4 + O_2$). The fast O_2-evolution rate and the highest O_2 yield of 100% (5.0 µmol) were achieved for the reaction systems employing Ca^{2+} and Sc^{3+}-incorporated Co cyanide complexes as the WOCs. Incorporation effect of Sc^{3+} ion is similar to that of Ca^{2+} ion, however, the complexes incorporating Ca^{2+} ion were mainly investigated, because Ca^{2+} ion is an earth abundant element

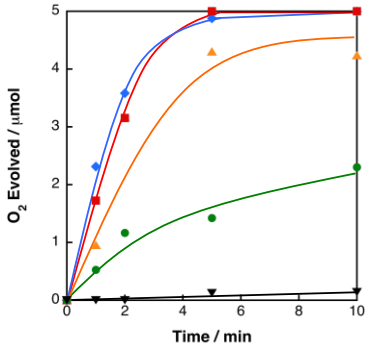

Fig. 3 Time courses of O_2 evolution by visible-light irradiation (λ > 420 nm) of a phosphate buffer (2.0 mL, 50 mM, pH 7.0) containing $[Ru(bpy)_3]^{2+}$ (1.0 mM), $Na_2S_2O_8$ (5.0 mM) and a WOC (80 μg), $Ca_{0.06}[Co^{II}(H_2O)_2]_{1.44}[Co^{III}(CN)_6]$ (red square), $Sc_{0.08}[Co^{II}(H_2O)_2]_{1.38}[Co^{III}(CN)_6]$ (blue diamond), $Mg_{0.05}[Co^{II}(H_2O)_2]_{1.45}[Co^{III}(CN)_6]$ (orange triangle), $[Co^{II}(H_2O)_2]_{1.50}[Co^{III}(CN)_6]$ (green circle)]. The black inverse triangles are the data obtained without catalyst.

and also used in natural photosynthesis systems.

When the amount of incorporated Ca^{2+} ion was changed in $Ca_x[Co^{II}(H_2O)_2]_{1.5-x}[Co^{III}(CN)_6]$ (x = 0.06-0.37), the highest catalytic activity was obtained at x = 0.06 (Fig. S8†). The catalytic activity and the O_2 yield increased with increasing pH from 6.0 to 8.0 (Fig. S9†). The quantum efficiencies for the photocatalytic O_2 evolution with various amounts of $Ca_{0.06}[Co^{II}(H_2O)_2]_{1.44}[Co^{III}(CN)_6]$ were determined by using monochromatic light (λ = 450 nm) and actinometer at pH 7.0 as shown in Fig. 4a (see Experimental section† and Fig. S10†). The quantum efficiency increased with increasing the amount of the WOC to reach the maximum value (200%) as shown in Fig. 4b.

The highest catalytic activity was obtained for $Ca_{0.06}[Co^{II}(H_2O)_2]_{1.44}[Co^{III}(CN)_6]$, however, further increase in Ca^{2+} contents in $Ca_x[Co^{II}(H_2O)_2]_{1.5-x}[Co^{III}(CN)_6]$ resulted in lower initial O_2-evolution rates and yields. Differential pulse voltammetry (DPV) measurements manifested that the oxidation potentials of $Ca_x[Co^{II}(H_2O)_2]_{1.5-x}[Co^{III}(CN)_6]$ increased in proportion to the Ca^{2+} contents from 1.07 to 1.16 V (Fig. 5). Although the higher oxidation potentials were achieved at higher Ca^{2+} contents, the activity for photocatalytic water oxidation was not further enhanced. This is probably due to a decrease in the number of Co^{II} ions, which not only act as

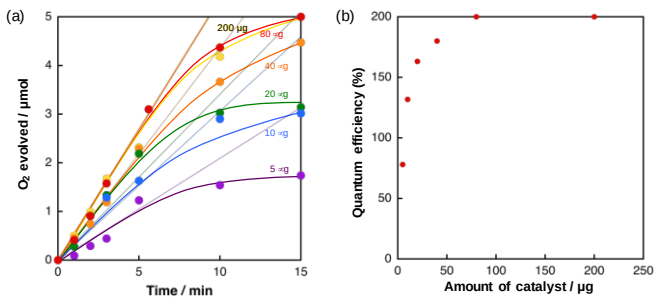

Fig. 4 (a) Time courses of O_2 evolution by photoirradiation (λ = 450 nm) of a phosphate buffer (2.0 mL, 50 mM, pH 7.0) containing various amounts of $Ca_{0.06}[Co(H_2O)_2][Co(CN)_6]$ (5 – 80 μg), $[Ru(bpy)_3]^{2+}$ (1.0 mM, 1.6 mg), $Na_2S_2O_8$ (5.0 mM, 2.4 mg) in a quartz cuvette (light path length: 1.0 cm). (b) Plot of the quantum efficiency vs. the amount of the catalyst, $Ca_{0.06}[Co(H_2O)_2][Co(CN)_6]$.

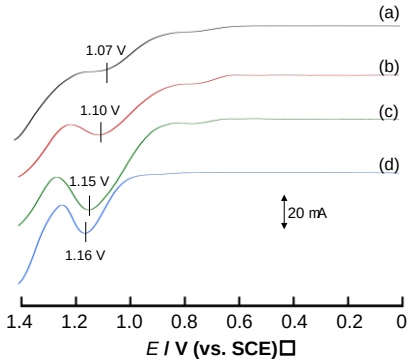

Fig. 5 Differential pulse voltammograms of $Ca_x[Co^{II}(H_2O)_2]_{1.5-x}$-$[Co^{III}(CN)_6]$. x = (a) 0, (b) 0.06 and (c) 0.14 and (d) 0.37. The measurements were performed in a phosphate buffer (2.0 mL, 50 mM, pH 7.0) suspension of $Ca_x[Co^{II}(H_2O)_2]_{1.5-x}[Co^{III}(CN)_6]$ (1.0 μmol) using a glassy carbon electrode, a Pt wire and a saturated calomel electrode as a working electrode, an auxiliary counter electrode and a reference electrode, respectively.

active sites for water oxidation but also provide water nests for incorporating Ca^{2+} ions, by increasing the Ca^{2+} contents.

DPV measurements of the Mg^{2+} and Sc^{3+} incorporated complexes also showed positive shift of the oxidation potentials (Fig. 6). The oxidation potentials were more positively shifted by increasing the amounts of Mg^{2+} and Sc^{3+} ions, confirming their incorporation in the complexes, however, no direct correlation was found between the redox potential and catalytic activity (Figs. S11 and S12†).

The robustness of $Ca_{0.06}[Co^{II}(H_2O)_2]_{1.44}[Co^{III}(CN)_6]$ was evidenced by no significant change in the composition determined by XRF and the structure examined by XRD and IR after reactions (Figs. S13 and S14†). However, successive addition of a small aliquot of a concentrated $Na_2S_2O_8$ solution to the reaction solution after O_2 evolution ceased resulted in a decrease in the amount of O_2 evolution (Fig. S15†), probably because of decomposition of the ligand of $[Ru^{II}(bpy)_3]^{2+}$ by decrease in pH in the solution during the reaction,[15] or partial decomposition of $Ca_{0.06}[Co^{II}(H_2O)_2]_{1.44}[Co^{III}(CN)_6]$.

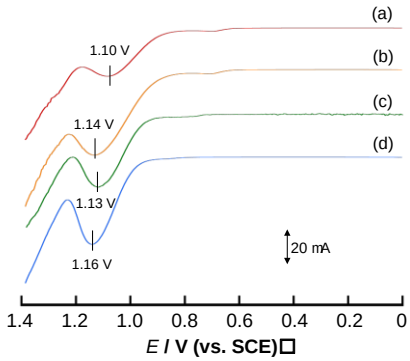

Fig. 6 Differential pulse voltammograms of $Mg_x[Co^{II}(H_2O)_2]_{1.5-x}$-$[Co^{III}(CN)_6]$ [x = (a) 0.05 and (b) 0.17] and $Sc_x[Co^{II}(H_2O)_2]_{1.5-1.5x}$- $[Co^{III}(CN)_6]$ [x = (c) 0.08 and (d) 0.12]. The measurements were performed in a phosphate buffer (2.0 mL, 50 mM, pH 7.0) suspension of $Mg_x[Co^{II}(H_2O)_2]_{1.5-x}[Co^{III}(CN)_6]$ or $Sc_x[Co^{II}(H_2O)_2]_{1.5-1.5x}[Co^{III}(CN)_6]$ (1.0 μmol) using a glassy carbon electrode, a Pt wire and a saturated calomel electrode as a working electrode, an auxiliary counter electrode and a reference electrode, respectively.

Conclusions

Incorporation of a small amount of Ca^{2+} ion into a polymeric Co cyanide complex ($Ca_{0.06}[Co^{II}(H_2O)_2]_{1.44}[Co^{III}(CN)_6]$) resulted in significant enhancement of the catalytic activity for the photocatalytic water oxidation by persulphate with $[Ru^{II}(bpy)_3]^{2+}$ to achieve the maximum quantum efficiency of 200% for the O_2 evolution as well as 100% O_2 yield in neutral water (pH 7.0). Incorporation of other redox-inactive metal ions to the polymeric Co cyanide complex also resulted in enhancement of the catalytic activity for the photocatalytic water oxidation. Thus, incorporation of redox-inactive metal ions as Lewis acids, which can interact with catalytically active sites for water oxidation through coordinating water molecules, is a promising method to achieve the maximum quantum efficiency for the photocatalytic water oxidation.

Acknowledgements

The authors acknowledge Mr. Masatsugu Ishimoto for TEM measurements. This work was supported by the SENTAN project from Japan Science Technology Agency (JST) to S.F., Grants-in-Aid (no. 16H02268 to S.F., no. 15K14223 to Y.Y.) for Scientific Research from Japan Society for the Promotion of Science (JSPS) and ENEOS hydrogen trust fund to Y. Y.

Notes and References

1 (*a*) L. Duan, L. Wang, F. Li, F. Li and L. Sun, *Acc. Chem. Res.*, 2015, **48**, 2084-2096; (*b*) D. K. Bediako, A. M. Ullman and D. G. Nocera, *Top. Curr. Chem*., 2016, **371**, 173-214; (*c*) K. J. Young, B. J. Brennan, R. Tagore and G. W. Brudvig, *Acc. Chem. Res.*, 2015, **48**, 567-574; (*d*) M. Zhang, H. Frei, *Catal. Lett.*, 2015, **145**, 420-435.

2 (*a*) R. L. House, N. Y. M. Iha, R. L. Coppo, L. Alibabaei, B. D. Sherman, P. Kang, M. K. Brennaman, P. G. Hoertz and T. J. Meyer, *J. Photochem. Photobiol., C*, 2015, **25**, 32-45; (*b*) J. D. Blakemore, R. H. Crabtree and G. W. Brudvig, *Chem. Rev.*, 2015, **115**, 12974-13005; (*c*) S. Berardi, S. Drouet, L. Francàs, C. Gimbert-Suriñach, M. Guttentag, C. Richmond, T. Stoll and A. Llobet, *Chem. Soc. Rev.*, 2014, **43**, 7501-7519.

3 (*a*) M. M. Najafpour, G. Renger, M. Holynska, A. N. Moghaddam, E.-M. Aro, R. Carpentier, H. Nishihara, J. J. Eaton-Rye, J.-R. Shen and S. I. Allakhverdiev, *Chem. Rev.*, 2016, **116**, 2886-2936; (*b*) J. R. Swierk and T. E. Mallouk, *Chem. Soc. Rev.*, 2013, **42**, 2357-2387; (*c*) S. Fukuzumi, J. Jung, Y. Yamada, T. Kojima and W. Nam, *Chem. Asian J.*, 2016, **11**, 1138 – 1150; (*d*) L. Chen, G. Chen, C.-F. Leung, S.-M. Yiu, C.-C. Ko, E. Anxolabéhère-Mallart, M. Robert and T.-C. Lau, *ACS Catal.*, 2015, **5**, 356-364.

4 (*a*) Y. Umena, K. Kawakami, J.-R. Shen and N. Kamiya, *Nature*, 2011, **473**, 55–60; (*b*) M. Suga, F. Akita, K. Hirata, G. Ueno, H. Murakami, Y. Nakajima, T. Shimizu, K. Yamashita, M. Yamamoto, H. Ago and J.-R. Shen, *Nature*, 2015, **517**, 99-103.

5 I. Ugur, A. W. Rutherford and V. R. I. Kaila, *Biochim. Biophys. Acta Bioenerg.*, 2016, **1857**, 740-748.

6 (*a*) V. Krewald, F. Neese and D. A. Pantazis, *Phys. Chem. Chem. Phys.*, 2016, **18**, 10739-10750; (*b*) J. S. Kanady, E. Y. Tsui, M. W. Day and T. Agapie, *Science*, 2011, **333**, 733-736.

7 K. Yamaguchi, S. Yamanaka, H. Isobe, T. Saito, K. Kanda, Y. Umena, K. Kawakami, J.-R. Shen, N. Kamiya, M. Okumura, H. Nakamura, M. Shoji and Y. Yoshioka, *Int. J. Quantum Chem.*, 2013, **113**, 453-473.

8 (*a*) V. K. Yachandra and J. Yano, *J. Photochem. Photobiol., B.*, 2011, **104**, 51-59; (*b*) N. Ishida, M. Sugiura, F. Rappaport, T.-L. Lai, A. W. Rutherford and A. Boussac, *J. Biol. Chem.*, 2008, **283**, 13330-13340; (*c*) J. P. McEvoy and G. W. Brudvig, *Phys. Chem. Chem. Phys.*, 2004, **6**, 4754-4763.

9 J. Kim, X. Yin, K.-C. Tsao, S. Fang and H. Yang, *J. Am. Chem. Soc.*, 2014, **136**, 14646-14649.

10 (*a*) D. González-Flores, I. Zaharieva, J. Heidkamp, P. Chernev, E. Martínez-Moreno, C. Pasquini, M. R. Mohammadi, K. Klingan, U. Gernet, A. Fischer and H. Dau, *ChemSusChem*, 2016, **9**, 379-387; (*b*) C. Zhang, C. Chen, H. Dong, J.-R. Shen, H. Dau and J. Zhao, *Science*., 2015, **348**, 690-693.

11 (*a*) C. E. Frey, M. Wiechen and P. Kurz, *Dalton Trans.*, 2014, **43**, 4370-4379; (*b*) Y.-G. Lin, Y.-C. Chen, J. T. Miller, L.-C. Chen, K.-H. Chen and Y.-K. Hsu, *ChemCatChem*, 2014, **6**, 1684-1690; (*c*) F. Rong, J. Zhao, Z. Chen, Y. Xu, Y. Zhao, Q. Yang and C. Li, *J. Mater. Chem. A* 2016, **4**, 6585-6594.

12 (*a*) M. Wiechen, I. Zaharieva, H. Dau and P. Kurz, *Chem. Sci.* 2012, **3**, 2330-2339; (*b*) J. Y. C. Chen, J. T. Miller, J. B. Gerken and S. S. Stahl, *Energy Environ. Sci.*, 2014, **7**, 1382-1386; (*c*) Y. Guo, Y. Tong, P. Chen, K. Xu, J. Zhao, Y. Lin, W. Chu, Z. Peng and C. Wu, Y. Xie, *Adv. Mater.*, 2015, **27**, 5989-5994.

13 (*a*) E. Y. Tsui and T. Agapie, *Proc. Natl. Acad. Sci. U. S. A.*, 2013, **110**, 10084-10088; (*b*) B. Gerey, E. Goure, J. Fortage, J. Pecaut and M.-N. Collomb, *Coord. Chem. Rev.*, 2016, **319**, 1-24.

14 (*a*) S. Bang, Y.-M. Lee, S. Hong, K.-B. Cho, Y. Nishida, M. S. Seo, R. Sarangi, S. Fukuzumi and W. Nam, *Nat. Chem.*, 2014, **6**, 934-940; (*b*) S. Fukuzumi, Y. Morimoto, H. Kotani, P. Naumov, Y.-M. Lee and W. Nam, *Nat. Chem.*, 2010, **2**, 756-759; (*c*) S. Fukuzumi, K. Ohkubo, Y.-M. Lee and W. Nam, *Chem.–Eur. J.*, 2015, **21**, 17548-17559.

15 S. Fukuzumi, J. Jung, Y. Yamada, T. Kojima and W. Nam, *Chem. Asian J.*, 2016, **11**, 1138-1150.

16 (*a*) A. Sartorel, M. Bonchio, S. Campagna and F. Scandola, *Chem. Soc. Rev.*, 2013, **42**, 2262-2280; (*b*) A. Lewandowska-Andralojc and D. E. Polyansky, *J. Phys. Chem. A*, 2013, **117**, 10311-10319.

17 (*a*) F. Bolletta, A. Jurius, M. Maestri and D. Sandrini, *Inorg. Chim. Acta*, 1980, 44, L175-L176; (b) S. Fukuzumi, T. Kishi, H. Kotani, Y.-M. Lee and W. Nam, *Nat. Chem.*, 2011, **3**, 38-41.

18 (*a*) T. Zhang and W. Lin, *Chem. Soc. Rev.*, 2014, **43**, 5982-5993; (*b*) S. Goberna-Ferrón, W. Y. Hernández, B. Rodríguez-García and J. R. Galán-Mascarós, *ACS Catal.*, 2014, **4**, 1637-1641; (*c*) S. Pintado, S. Goberna-Ferrón, E. C. Escudero-Adan and J. R. Galán-Mascarós, *J. Am. Chem. Soc.*, 2013, **135**, 13270-13273.

19 (*a*) Y. Yamada, K. Oyama, R. Gates and S. Fukuzumi, *Angew. Chem., Int. Ed.*, 2015, *54*, 5613-5617; (*b*) Y. Isaka, K. Oyama, Y. Yamada, T. Suenobu and S. Fukuzumi, *Catal. Sci. Technol.*, 2016, **6**, 681-684.

20 (*a*) G. W. Beall, W. O. Milligan, J. Korp and I. Bernal, *Inorg. Chem.*, 1977, **16**, 2715-2718; (*b*) A. Flambard, F. H. Köhler and R. Lescouëzec, *Angew. Chem., Int. Ed.*, 2009, **48**, 1673-1676; (*c*) M. Schwarten and D. Z. Babel, *Anorg. Allg. Chem.*, 2000, **626**, 1921-1928.

21 (*a*) H. J. Buser, D. Schwarzenbach, W. Petter and A. Ludi, *Inorg. Chem.*, 1977, **16**, 2704-2710; (*b*) D. F. Mullica, J. D. Oliver, W. O. Milligan and F. W. Hills, *Inorg. Nucl. Chem. Lett.*, 1979, **15**, 361-365.

22 R. D. Shannon, *Acta Crystallogr., Sect. A: Cryst. Phys., Diffr., Theor. Gen. Crystallogr.*, 1969, **32**, 751-767.

23 K. Nakamoto, *Infrared and Raman Spectra of Inorganic and Coordination Compounds*, *Fourth Edition*, A Wiley-Interscience Publications, New York, 1986.

TOC Entry

Enhancement of Catalytic Activity by Lewis Acid

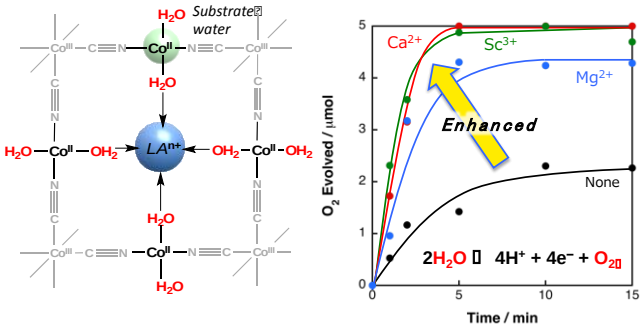

Water Oxidation Catalyst: $(LA)_x[Co(H_2O)_2]_y[Co(CN)_6]$ (LA: Lewis Acid)

Incorporation of a small amount of Ca^{2+} ion into a polymeric Co cyanide complex enhanced the catalytic activity for photocatalytic water oxidation by persulphate with $[Ru(bpy)_3]^{2+}$ at pH 7.0 to achieve the maximum quantum efficiency of 200%.